Journal of Visualized Experiments

Near-infrared temperature measurement technique for water surrounding an induction-heated small magnetic sphere

--Manuscript Draft--

Article Type:	Invited Methods Article - JoVE Produced Video
Manuscript Number:	JoVE57407R2
Full Title:	Near-infrared temperature measurement technique for water surrounding an induction-heated small magnetic sphere
Keywords:	Near-infrared imaging; temperature; induction heating; water; absorbance; magnetic sphere.
Corresponding Author:	Naoto KAKUTA, Ph.D. Tokyo Metropolitan University Hachioji, Tokyo JAPAN
Corresponding Author's Institution:	Tokyo Metropolitan University
Corresponding Author E-Mail:	kakuta-n@tmu.ac.jp
First Author:	Naoto Kakuta
Other Authors:	Keisuke Nishijima
	Cuong Van Han
	Yuki Arakawa
	Katsuya Kondo
	Yukio Yamada
Author Comments:	The submitted paper is based on our previous paper (J. Appl. Phys. 122, 044901, 2017). So the method is the same, but the text is different and the results are new ones. In our previous paper, the estimation method of the heat generation rate of the sphere is presented. However, this part is cut in the submitted paper, and the temperature imaging is focused on.
Additional Information:	
Question	**Response**
If this article needs to be "in-press" by a certain date, please indicate the date below and explain in your cover letter.	

January 24th, 2018

Dear Dr. Jialan Zhang:

I wish to submit the 2nd-revised article for publication in *Journal of Visualized Experiments (JoVE)*, titled "Near-infrared temperature measurement technique for water surrounding an induction-heated small magnetic sphere." According to the editors' comments, we have revised the corresponding parts.

Thank you for your consideration.

Sincerely yours,

Naoto Kakuta
Tokyo Metropolitan University
1-1 Minami-osawa, Hachioji, Tokyo, 192-0397 Japan
Phone: +81-426772706
Fax: +81-426772706
Email address: kakuta-n@tmu.ac.jp

TITLE:

Near-Infrared Temperature Measurement Technique for Water Surrounding an Induction-heated Small Magnetic Sphere

AUTHORS & AFFILIATIONS:

Naoto Kakuta[1], Keisuke Nishijima[1], Van Cuong Han[1], Yuki Arakawa[1], Katsuya Kondo[2], Yukio Yamada[3]

[1]Department of Mechanical Engineering, Tokyo Metropolitan University, Hachioji, Tokyo, Japan
[2]Department of Electrical and Electronic Engineering, Tottori University, Tottori, Japan
[3]Brain Science Inspired Life Support Research Center, The University of Electro-Communications, Chofu, Tokyo, Japan

CORRESPONDING AUTHOR:

Naoto Kakuta (kakuta-n@tmu.ac.jp)
Tel: +81-42-677-2706

EMAIL ADDRESSES OF CO-AUTHORS:

Keisuke Nishijima (nishijima-keisuke@ed.tmu.ac.jp)
Van Cuong Han (han-van-cuong@ed.tmu.ac.jp)
Yuki Arakawa (arakawa-yuki@ed.tmu.ac.jp)
Katsuya Kondo (kondo@eecs.tottori-u.ac.jp)
Yukio Yamada (yukioyamada@uec.ac.jp)

KEYWORDS:

Near-infrared imaging, temperature, induction heating, water, absorbance, magnetic sphere.

SUMMARY:

A technique utilizing wavelengths of 1150 and 1412 nm to measure the temperature of water surrounding an induction-heated small magnetic sphere is presented.

ABSTRACT:

A technique to measure the temperature of water and non-turbid aqueous media surrounding an induction-heated small magnetic sphere is presented. This technique utilizes wavelengths of 1150 and 1412 nm, at which the absorption coefficient of water is dependent on temperature. Water or a non-turbid aqueous gel containing a 2.0-mm- or 0.5-mm-diameter magnetic sphere is irradiated with 1150 nm or 1412 nm incident light, as selected using a narrow bandpass filter; additionally, two-dimensional absorbance images, which are the transverse projections of the absorption coefficient, are acquired via a near-infrared camera. When the three-dimensional distributions of temperature can be assumed to be spherically symmetric, they are estimated by applying inverse Abel transforms to the absorbance profiles. The temperatures were observed to consistently change according to time and the induction heating power.

INTRODUCTION:

A technique to measure temperature near a small heat source within a medium is required in many scientific research fields and applications. For example, in the research on magnetic hyperthermia, which is a cancer therapy method using electromagnetic induction of magnetic particles, or small magnetic pieces, it is critical to accurately predict the temperature distributions generated by the magnetic particles[1,2]. However, although microwave[3,4], ultrasound[5-8], optoacoustic[9], Raman[10], and magnetic resonance[11,12]-based temperature measurement techniques have been researched and developed, such an inner temperature distribution cannot be accurately measured at present. Thus far, single-position temperatures or temperatures at a few positions have been measured via temperature sensors, which, in the case of induction heating, are non-magnetic optical fiber temperature sensors[13,14]. Alternatively, the surface temperatures of media have been remotely measured via infrared radiation thermometers to estimate the inner temperatures[14]. However, when a medium containing a small heat source is a water layer or a non-turbid aqueous medium, we have demonstrated that a near-infrared (NIR) absorption technique is useful to measure the temperatures[15–19]. This paper presents the detailed protocol of this technique and representative results.

The NIR absorption technique is based on the principle of temperature dependence of the absorption bands of water in the NIR region. As is shown in **Figure 1a**, the $\nu_1 + \nu_2 + \nu_3$ absorption band of water is observed in the 1100-nm to 1250-nm wavelength (λ) range and shifts to shorter wavelengths as the temperature increases[19]. Here, $\nu_1 + \nu_2 + \nu_3$ means that this band corresponds to the combination of the three fundamental O–H vibration modes: symmetric stretching (ν_1), bending (ν_2), and antisymmetric stretching (ν_3)[20,21]. This change in the spectrum indicates that the most temperature-sensitive wavelength in the band is $\lambda \approx 1150$ nm. Other absorption bands of water also exhibit similar behavior with respect to the temperature[15–18,20,21]. The $\nu_1 + \nu_3$ band of water observed within the range λ = 1350−1500 nm and its temperature dependence are shown in **Figure 1b**. In the $\nu_1 + \nu_3$ band of water, 1412 nm is the most temperature-sensitive wavelength. Thus, it is possible to obtain two-dimensional (2D) temperature images by using an NIR camera to capture 2D absorbance images at λ = 1150 or 1412 nm. As the absorption coefficient of water at λ = 1150 nm is smaller than that at λ = 1412 nm, the former wavelength is suitable for approximately 10-mm-thick aqueous media, while the latter is suitable for approximately 1-mm-thick ones. Recently, using λ = 1150 nm, we obtained the temperature distributions in a 10-mm-thick water layer containing an induction-heated 1-mm-diameter steel sphere[19]. Moreover, the temperature distributions in a 0.5-mm-thick water layer have been measured by using λ = 1412 nm[15,17].

An advantage to the NIR-based temperature imaging technique is that it is simple to setup and implement because it is a transmission-absorption measurement technique and needs no fluorophore, phosphor, or other thermal probe. In addition, its temperature resolution is less than 0.2 K[15,17,19]. Such a good temperature resolution cannot be achieved by other transmission techniques based on interferometry, which have often been used in heat and mass transfer studies[22-24]. We note, however, that the NIR-based temperature imaging technique is not suitable in cases with considerable local temperature change, because the deflection of light caused by the large temperature gradient becomes dominant[19]. This matter is referred in this paper in terms of practical use.

This paper describes the experimental setup and procedure for the NIR-based temperature imaging technique for a small magnetic sphere heated via induction; additionally, it presents the results of two representative 2D absorbance images. One image is of a 2.0-mm-diameter steel sphere in a 10.0-mm-thick water layer that is captured at λ = 1150 nm. The second image is of a 0.5-mm-diameter steel sphere in a 2.0-mm-thick maltose syrup layer that is captured at λ = 1150 nm. This paper also presents the calculation method and results of the three-dimensional (3D) radial distribution of temperature by applying the inverse Abel transform (IAT) to the 2D absorbance images. The IAT is valid when a 3D temperature distribution is assumed to be spherically symmetric as in the case of a heated sphere (**Figure 2**)[19]. For the IAT calculation, a multi-Gaussian function fitting method is employed here, because the IATs of Gaussian functions can be obtained analytically[25-29] and fit well to monotonically decreasing data; this includes experiments employing thermal conduction from a single heat source.

PROTOCOL:

1. Experimental Setup and Procedures

Prepare an optical rail to mount a sample and optics for NIR imaging as follows.

1.1. Sample preparation.

Note: When using water or aqueous liquid, do Step 1.1.1. When using an aqueous gel with high viscosity, do Step 1.1.2.

1.1.1. Steel sphere setting in water.

1.1.1.1. Fix a 2.0-mm-diameter steel sphere to the end of a thin plastic string using a small amount of glue.

1.1.1.2. Hang the steel sphere at the center of the rectangular glass cell with an optical path length of 10.0 mm, a width of 10 mm, and a height of 45 mm (**Figure 3**).

1.1.1.3. Pour filtered water into the cell carefully so as not to produce air bubbles.

Note: A steel sphere can also be fixed to the tip of a thin plastic rod with a small amount of glue[19].

1.1.2. Steel sphere setting in aqueous gel.

1.1.2.1. Heat an aqueous gel to reduce its viscosity such that it is low enough to be poured smoothly.

1.1.2.2. Using a syringe, pour the aqueous gel into a rectangular glass cell with an optical path length of 2.0 mm, a width of 10 mm, and a height of 45 mm to half-full and leave it to cool.

1.1.2.3. Place a 0.5-mm-diameter steel sphere in the center of the gel surface.

1.1.2.4. Fill the cell with the aqueous gel.

Note: Larger spheres (>~1 mm dia.) should not be used with a gel because they will move by gravitational and/or magnetic forces during induction heating.

1.1.3. Set the cell in a plastic holder and mount it on the optical rail (**Figure 3**).

1.2. Preparation of NIR imaging system.

1.2.1. Prepare a halogen lamp with a fiber light guide, and fix the end of the fiber light guide with a holder on the optical rail.

1.2.2. Place a narrow bandpass filter (NBPF) with a transmittance peak at λ = 1150 nm or λ = 1412 nm between the fiber light guide and the cell (**Figure 3**).

1.2.3. Interpose another bandpass filter (BPF), whose transmission wavelength range is wider than that of the NBPF, between the halogen lamp and the NBPF.

Note: The BPF is needed to prevent thermal damage to the NBPF because it receives light directly.

1.2.4. Interpose an iris diaphragm(s) in the light path between the NBPF and cell holder to reduce the stray light (**Figure 3**).

1.2.5. Set up an NIR camera to detect the light transmitted through the cell (**Figure 3**). Connect the camera through a data transfer cable to a graphic board installed in a personal computer (PC) with image acquisition software.

1.2.6. Set a telecentric lens between the cell and camera (**Figure 3**).

Note: A common camera lens can also be used. However, a telecentric lens is better in terms of the selective detection of the light parallel to the chief ray for the IAT and reduction of the influence of diffraction.

Note: The NBPF and BPF should not be placed between the cell and camera because, in doing so, the water temperature would increase via direct absorption of high-intensity light from the halogen lamp.

1.2.7. Turn on the NIR camera and launch the image acquisition software.

1.2.8. Light the halogen lamp and adjust its output power observing the image displayed on the monitor (**Figure 4**).

1.2.9. Adjust the axis, position, and focus of the telecentric lens to obtain a fine image of the steel

sphere.

Note: If the adjustment is not complete, irregular intensity patterns will appear, leading to incorrect absorbances.

1.3. Preparation of induction heating system.

1.3.1. Prepare an induction heating system consisting of a high-frequency generator (maximum output power: 5.6 kW; frequency: 780 kHz), water-cooled coil, and water chiller.

Note: An induction heating system for brazing, welding, and soldering small metal parts is appropriate for this purpose; see **Table of Materials**.

1.3.2. If possible, mount the coil on an XYZ movable stage to change its position.

1.3.3. Place the coil near the cell such that the distance between the coil center and the steel sphere is approximately 15 mm (**Figure 3**). Ensure that there are no other metal parts near the coil.

Note: The distance should be adjusted depending on the induction heating power and the sphere size.

1.3.4. Circulate water for cooling.

1.4. Image acquisition and induction heating.

1.4.1. Click “start” on the image acquisition software to store the images sequentially.

1.4.2. Click “start” on the induction heating control software to commence the induction heating.

1.4.3. After several seconds (depending on the conditions and purpose), click “stop” on the image acquisition software.

1.4.4. Click “stop” on the induction heating control software.

1.4.5. Save the temporally-stored images as a TIFF sequence (or other non-compressed format) on the image acquisition software.

Note: If the temperature is high enough, the effect of light deflection will appear on the image[7]. The induction heating power must be decreased appropriately though experiments such that the increase in the temperature near the sphere is less than approximately 10 K, which can be confirmed in the following protocol steps for temperature estimation.

2. Image Processing and Temperature Estimation

Note: The saved sequential images are represented as $I_i(x, z)$, where i is the sequential frame number. The coordinates, x, y, z, r, and r' are defined as are indicated in **Figure 2**; z is positive in the direction opposite to gravity. The outline of the following protocol steps is also illustrated in **Supplement 1**.

2.1. Absorbance image construction.

2.1.1. Open $I_i(x, z)$ with the image processing software.

2.1.2. Reduce noise in $I_i(x, z)$ by implementing 3 × 3 pixel averaging.

2.1.3. Create an average image of $I_i(x, z)$ over i = 1 to 5 (or more) before heating, and define it as the reference image, $I_r(x, z)$.

Note: This averaging reduces the noise to obtain a more reliable image than a single frame image.

2.1.4. Construct the sequential images of the absorbance difference, $\Delta A_i(x, z)$, via the following equation:

$$\Delta A_i(x, z) = -\log_{10} \frac{I_i(x, z)}{I_r(x, z)}. \quad (1)$$

Note: $\Delta A_i(x, z)$ is the variation in the absorbance, $A_i(x, z)$, from the reference absorbance, $A_r(x, z)$, before heating, and is derived as follows[15-19]:

$$\Delta A_i = A_i - A_r = -\log_{10} \frac{I_i}{I_0} - \left(-\log_{10} \frac{I_r}{I_0} \right) = -\log_{10} \frac{I_i}{I_r}, \quad (2)$$

where I_0 is the intensity of incident light to the cell.

2.1.5. Colorize the ΔA_i images using an appropriate color map such as blue-to-red.

Note: The command script file for running Steps 2.1.2 through 2.1.5 for ImageJ is presented in **Supplement 2**.

2.2. Temperature estimation.

2.2.1. Choose the time period during which $\Delta A_i(x, z)$ is circularly symmetric with respect to the center of the sphere by visually observing the images.

Note: The circular symmetry is broken mainly by free convection. An image-based analytical judgement of free convection occurring is introduced in the previous work[19]; however,

practically, the visual judgement is effective.

2.2.2. Extract the $\Delta A_i(r', \vartheta)$ data along 360 radial lines ($\Delta\vartheta = 1^\circ$) on the $\Delta A_i(x, z)$ images.

2.2.3. Exclude the $\Delta A_i(r', \vartheta)$ data within the sphere and in its vicinity ($\Delta r' \approx 0.2$ mm). Note: The data are anomalously very small or large in the vicinity mainly because of the slight movement of the sphere.

2.2.4. Average $\Delta A_i(r', \vartheta)$ over ϑ to determine the line profile, $\Delta A_i(r')$.

Note: The command script file for running Steps 2.2.2 through 2.2.4 for ImageJ is presented in **Supplement 3**.

2.2.5. Approximate the $\Delta A_i(r')$ data by the following multi-Gaussian function:

$$\Delta A_i(r') = \sum_{j=1}^{N} a_j \left[\exp\left(-\frac{r'^2}{\sigma_j^2} \right) - \exp\left(-\frac{R^2}{\sigma_j^2} \right) \right], \tag{3}$$

where a_j is the weighting factor, σ_j is the dispersion parameter, and R is the maximum of r' where $\Delta A_i(R) = 0$ can be assumed.

2.2.6. Calculate the absorption coefficient difference, $\Delta\mu_i(r)$, by substituting the obtained N, a_j, and σ_j into the following IAT of Eq. (3):

$$\Delta\mu_i(r) = \sum_{j=1}^{N} \frac{1}{\sqrt{\pi}} \frac{a_j}{\sigma_j} \exp\left(-\frac{r^2}{\sigma_j^2} \right) \operatorname{erf}\left(\frac{\sqrt{R^2 - r^2}}{\sigma_j} \right), \tag{4}$$

where erf is the error function.

2.2.7. Convert $\Delta\mu_i(r)$ to temperature via the following equation:

$$\Delta T_i(r) = \frac{\Delta\mu_i(r)}{\alpha_f} \tag{5}$$

with the temperature coefficients of water, α_f, which are 4.0×10^{-3} K^{-1} mm^{-1} for $\lambda = 1150$ nm[19] and 4.1×10^{-3} K^{-1} mm^{-1} for $\lambda = 1412$ nm[17].

Note: The command script file for running Steps 2.2.5 through 2.2.7 is presented in **Supplement 4**, where the Levenberg–Marquardt nonlinear least-squares algorithm[17,19] is employed for Step 2.2.5.

REPRESENTATIVE RESULTS:

Images of $\Delta A_i(x, z)$ at λ = 1150 nm for a 2.0-mm-diameter steel sphere in water and at λ = 1412 nm for a 0.5-mm-diameter steel sphere in maltose syrup are presented in **Figure 5a** and **Figure 6a**, respectively. In both cases, the sphere was located 12 mm below the bottom of the coil along its central axis. **Figure 5b** and **Figure 6b** show the $\Delta A(r')$ data and their fitted multi-Gaussian functions in Eq. (3) with R = 3.0 mm and R = 1.5 mm, respectively. No more than two or three Gaussian functions (N = 2 or 3) are needed to achieve a good fit[17,19]. The fitted functions were then transformed into $\Delta T(r)$ profiles via Eqs. (4) and (5), and are presented in **Figure 5c** and **Figure 6c**.

The ΔA images in both cases clearly show an increase in the temperature of the water and gel surrounding the sphere due to thermal conduction. The circular symmetry of ΔA with respect to the sphere is observed in all images. The plots and curves in **Figure 5c** indicate that $\Delta A(r')$ increases with time at distances nearest to the sphere; at $r' \geq 2.5$ mm, no significant change is observed. Moreover, the $\Delta T(r)$ profiles obtained via the IAT verify the occurrence of thermal conduction in the radial direction. Note that, although the $\Delta T(r)$ profiles appear similar to those of $\Delta A(r')$, the changes in the $d\Delta T(r)/dr$ gradient differ from those of the $\Delta A(r')$ profiles. In **Figure 6**, the magnitudes of ΔA are found to correspond to the heating power levels, *i.e.,* heat generation rates of the sphere.

Results for the 0.5-mm-diameter sphere demonstrate that free convection, which distorts the circular pattern in ΔA, was not observed after t = 1.2 s. Conversely, for the 2.0-mm-diameter sphere in water, free convection was found to occur after t = 1.2 s (not shown). This means that a transition from a pure thermal conduction regime to a free convection regime may have occurred in the water at approximately t = 1.2 s. This difference in free convection was caused by the differences in the heat generation rate and viscosity. The heat generation rate of the 0.5-mm-diameter sphere was significantly smaller than that of the 2.0-mm-diameter sphere; furthermore, the viscosity of the maltose syrup (approximately 100 Pa·s) was considerably higher than that of water (approximately 0.001 Pa·s). Because free convection is an important topic in heat and mass transfer research, the proposed imaging technique, which provides the onset time of free convection and pattern of the thermal plume and yields information on the physical conditions inducing free convection, will contribute significantly to research in this field.

FIGURE AND TABLE LEGENDS:

Figure 1: Temperature dependence of NIR absorption spectrum of water. (a, b) Absorption band spectra of water at temperatures from 16.0 °C (blue) to 44.0 °C (red) in 4.0 °C increments in wavelength ranges of 1100–1250 nm and 1350–1500 nm, respectively. The arrows indicate the direction of the increase in temperature. The insets show the absorbance difference spectra; the absorbance spectra at 16.0 °C are the references. The optical path lengths are 10 mm and 1.0 mm in (a) and (b), respectively. The vertical dashed lines indicate the temperature-sensitive wavelengths of 1150 nm and 1412 nm used to obtain the NIR images.

Figure 2: Coordinate system and geometry for absorbance imaging. Reproduced from Kakuta *et al.* 2017[19] with the permission of AIP Publishing.

Figure 3: Experimental setup. (a) Schematic of the optical system and induction heating setup. See text for details. This figure has been modified from Kakuta *et al.* 2017[19] with the permission of AIP Publishing. (b) Photograph of the experimental setup. (c) Photograph showing a 2.0-mm-diameter steel sphere hung by a string, cell, and coil with a scale.

Figure 4: Acquired raw images. (a, b) Transmitted intensity images, $I(x, z)$, at λ = 1150 nm for a 2.0-mm-diameter steel sphere in water and λ = 1412 nm for a 0.5-mm-diameter steel sphere in maltose syrup, respectively.

Figure 5: Absorbance images and temperature profiles for a 2.0-mm-diameter steel sphere in water. (a) $\Delta A(x, z)$ images at λ = 1150 nm and t = 0.4, 0.8, and 1.2 s after the onset of induction heating. (b) Plots of $\Delta A(r')$ and their multi-Gaussian fits (solid curves). (c) $\Delta T(r)$ profiles obtained by performing IATs on $\Delta A(r')$.

Figure 6: Absorbance images and temperature profiles for a 0.5-mm-diameter steel sphere in maltose syrup. (a) $\Delta A(x, z)$ images at λ = 1412 nm and t = 0.4, 0.8, and 1.2 s after the onset of induction heating for the heating power levels of 10%, 30%, and 50%. (b) Plots of $\Delta A(r')$ and their multi-Gaussian fits (solid curves) for 50%. (c) $\Delta T(r)$ profiles obtained by performing IATs on $\Delta A(r')$ for 50%.

Supplement 1: Outline of image processing.

Supplement 2: Command script file for absorbance image construction (macro for ImageJ).

Supplement 3: Command script file for line profile extraction (macro for ImageJ).

Supplement 4: Matlab code for multi-Gaussian fitting and inverse Abel transform.

DISCUSSION:

The technique presented in this paper is a novel one using the temperature dependence of NIR absorption of water and presents no significant difficulty in setting up the necessary equipment and implementation. The incident light can be easily produced by using a halogen lamp and an NBPF. However, lasers cannot be used, because coherent interference patterns would appear on the images. Common optical lenses and glass cells for visible-light use can be used, as they transmit an adequate amount of light at λ = 1150 nm and 1412 nm. Additionally, InGaAs cameras can be purchased now at a relatively inexpensive price.

The NBPFs at λ = 1150 nm and 1412 nm are available by semi-custom order, but they are not excessively expensive. If there is a ready-made NBPF at a different wavelength, which must be within the temperature-dependent wavelength range (**Figure 1**), it can be used instead, although the temperature sensitivity, or α_f, might decrease. For example, the α_f value at λ = 1175 nm is one-half of that at λ = 1150 nm. Furthermore, the bandwidth or sharpness of the NBPF affects α_f; as the bandwidth increases, α_f decreases[15]. Thus, when the accurate estimation of $\Delta T(r)$ is

required, the transmittance spectrum of the NBPF should be measured by a spectrophotometer.

As mentioned in Step 1.4 of the protocol, because the refractive index of water varies with temperature, light rays passing through the temperature field around a sphere are deflected, causing changes in the $\Delta A(x, z)$ images. This problem was investigated in our previous work[19]. According to the results obtained via this study, as long as the maximum temperature near the sphere is moderately small (<10 K, approximately), the contribution of light deflection to the change in $\Delta A(x, z)$ can be negligible or sufficiently smaller than that of light absorption, because the light is incoherent and a certain deflection angle is accepted by the aperture stop of the telecentric lens; this means that the deflected rays pass though the aperture and focus on the same point in the image plane as the chief ray[30]. However, considering this, the aperture stop should be carefully adjusted such that the acceptance angle of the telecentric lens is slightly larger than the predicted deflection angle. Trial-and-error adjustments may be required for the initial experiment.

Image processing in Step 2.1 of the protocol and calculating IAT in Step 2.2 require no advanced mathematical knowledge. Step 2.1 can be performed easily with common image processing software that can treat TIFF sequence files. In Step 2.2.2, if the line profiles at multiple angles cannot be automatically obtained using command scripts, a single line profile extracted manually on image processing software can instead be used, although variations due to noises are not reduced.

When using an aqueous medium, its water content, or mole fraction, should be known or measured, especially for an accurate estimation of ΔT, because α_f depends on the water content. In other words, as the absorption coefficients of aqueous solutes and gel substrates depend little on temperature, the temperature sensitivity is almost proportional to the water content. If the water content is known to be very high, as with aqueous liquids, the α_f value of water given in this paper can be used practically. Otherwise, multiplying the α_f value of water by the predicted or measured water content, i.e., reducing α_f, may be effective for a sufficiently accurate estimation.

Considering the temperature detection limit (~0.2 K) and spatial resolution (~30 μm; this depends on pixel size and magnification), it is impossible for the presented technique to detect a minute temperature increase caused by single micro- and nano-magnetic particles heated inductively. However, if a large number of particles can be aggregated, contained in a capsule, or flowed in a thin tube, the temperature would increase over the detection level. In the research on magnetic hyperthermia, actually, such aggregation or selective adsorption of magnetic nanoparticles to cancer cells and the resulting temperatures are important and investigated. Hence, the presented technique is expected to be used for in vitro experiments in magnetic hyperthermia studies and other applications using magnetic particles. Spherical symmetry in the temperature distribution may not be obtained in these applications, but the 2D images will suffice to inform researchers about the temperature, the number and distribution of particles, and the heating performance.

The presented technique can be used to evaluate magnetic fields used in various magnetic applications[31,32]. Generally, magnetic fields produced by coils are very complicated, and cannot be precisely measured or theoretically predicted. However, as demonstrated in our previous work[19], the temperatures and heat generation rates of a magnetic sphere at different positions under different coil currents can be obtained by our technique. The spatial distribution of the heat generation rate must correspond to the magnetic field. Finally, the presented technique can be implemented, not only for electromagnetic induction, but also for ultrasound focusing, chemical reactions in droplets, and other local heating methods.

ACKNOWLEDGMENTS:

The authors thank Mr. Kenta Yamada, Mr. Ryota Fujioka, and Mr. Mizuki Kyoda for their support on the experiments and data analyses. This work was supported by JSPS KAKENHI Grant Number 25630069, the Suzuki Foundation, and the Precise Measurement Technology Promotion Foundation, Japan.

DISCLOSURES:

The authors have nothing to disclose.

REFERENCES:

1. Moros, E.G. (eds.) *Physics of Thermal Therapy*. CRC Press, 2012.
2. Périgo, E.A., Hemery, G., Sandre, O., Ortega, D., Garaio, E., Plazaola, F., Teran, F.J. Fundamentals and advances in magnetic hyperthermia. *Appl Phys Rev.* **2**, 041302 (2015).
3. Bardati, F., Marrocco, G., Tognolatti, P. Time-dependent microwave radiometry for the measurement of temperature in medical applications. *IEEE Trans Microwave Theo Tech*. **52**, 1917 –1924 (2004).
4. Levick, A., Land, D., Hand, J. Validation of microwave radiometry for measuring the internal temperature profile of human tissue. *Meas Sci Technol*. **22**, 065801 (2011).
5. Daniels, M.J., Varghese, T., Madsen, E.L., Zagzebski, J.A. Non-invasive ultrasound-based temperature imaging for monitoring radiofrequency heating—phantom results. *Phys Med Biol*. **52**, 4827 (2007).
6. Daniels, M.J., Varghese, T. Dynamic frame selection for in vivo ultrasound temperature estimation during radiofrequency ablation. *Phys Med Biol*. **55**, 4735 (2010).
7. Seo C.H., Shi, Y., Huang, S.-W., Kim, K., O'Donnell, M. Thermal strain imaging: A review. *Interface Focus* **1**, 649–664 (2011).
8. Bayat, M., Ballard, J.R., Ebbini E.S. Ultrasound thermography: A new temperature reconstruction model and in vivo results. *AIP Conf Proc*. **1821**, 060004 (2017).
9. Petrova, E., Liopo, A., Nadvoretskiy, V., Ermilov, S. Imaging technique for real-time temperature monitoring during cryotherapy of lesions. *J Biomed Opt*. **21**, 116007 (2016).
10. Gardner, B., Matousek, P., Stone, N. Temperature spatially offset Raman spectroscopy (T-SORS): Subsurface chemically specific measurement of temperature in turbid media using anti-Stokes spatially offset Raman spectroscopy. *Anal Chem*. **88**, 832–837 (2016).
11. Yoshioka, Y., Oikawa, H., Ehara, S., Inoue, T., Ogawa, A., Kanbara, Y., Kubokawa, M. Noninvasive measurement of temperature and fractional dissociation of imidazole in human lower leg muscles using ^{1}H-nuclear magnetic resonance spectroscopy. *J Appl Physiol*. **98**,

282–287 (2004).
12. Galiana, G., Branca, R.T., Jenista, E.R., Warren, W.S. Accurate temperature imaging based on intermolecular coherences in magnetic resonance, *Science.* **322**, 421–424 (2008).
13. Rapoport, E., Pleshivtseva, Y. *Optimal Control of Induction Heating Processes*. CRC Press. Boca Raton, FL. (2006).
14. Lucía, O., Maussion, P., Dede, E.J., Burdío, J.M. Induction heating technology and its applications: Past developments, current technology, and future challenges. *IEEE Trans Ind Electron*. **61**, 2509–2520 (2014).
15. Kakuta, N., Kondo, K., Ozaki, A., Arimoto, H., Yamada, Y. Temperature imaging of sub-millimeter-thick water using a near-infrared camera. *Int J Heat Mass Trans*. **52**, 4221–4228 (2009).
16. Kakuta, N., Fukuhara, Y., Kondo, K., Arimoto, H., Yamada, Y. Temperature imaging of water in a microchannel using thermal sensitivity of near-infrared absorption, *Lab Chip*. **11**, 3479–3486 (2011).
17. Kakuta, N., Kondo, K., Arimoto, H., Yamada, Y. Reconstruction of cross-sectional temperature distributions of water around a thin heating wire by inverse Abel transform of near-infrared absorption images. *Int J Heat Mass Trans*. **77**, 852–859 (2014).
18. Kakuta, N., Yamashita, H., Kawashima, D., Kondo, K., Arimoto, H., Yamada, Y. Simultaneous imaging of temperature and concentration of ethanol–water mixtures in microchannel using near-infrared dual-wavelength absorption technique. *Meas Sci Technol*. **27**, 115401 (2016).
19. Kakuta, N., Nishijima, K., Kondo, K., Yamada, Y. Near-infrared measurement of water temperature near a 1-mm-diameter magnetic sphere and its heat generation rate under induction heating. *J Appl Phys*. **122**, 044901 (2017).
20. Libnau, F.O., Kvalheim, O.M., Christy, A.A., Toft, J. Spectra of water in the near- and mid-infrared region, *Vib Spectrosc*. **7**, 243–254 (1994).
21. Siesler, H.W., Ozaki, Y., Kawata, S., Heise, H. M. *Near-Infrared Spectroscopy*. Wiley-VCH. (2002).
22. Shakher, C., Nirala, A.K. A review on refractive index and temperature profile measurements using laser-based interferometric techniques. *Opt Laser Eng*. **31**, 455–491 (1999).
23. Assebana, A., Lallemanda, M., Saulniera, J.-B., Fominb, N., Lavinskaja, E., Merzkirchc, W., Vitkinc, D. Digital speckle photography and speckle tomography in heat transfer studies. *Opt Laser Technol*. **32**, 583–592 (2000).
24. Ambrosini, D., Paoletti, D., Spagnolo, S.G. Study of free-convective onset on a horizontal wire using speckle pattern interferometry. *Int J Heat Mass Trans*. **46**, 4145–4155 (2003).
25. Bracewell, R. N. *The Fourier Transform and Its Applications*. McGraw-Hill. (2000).
26. Yoder, L.M., Barker, J.R., Lorenz, K.T., Chandler, D.W. Ion imaging the recoil energy distribution following vibrational predissociation of triplet state pyrazine–Ar van der Waals clusters. *Chem Phys Lett*. **302**, 602–608 (1999).
27. De Colle, F., de Burgo, C., Raga, A.C. Diagnostics of inhomogeneous stellar jets: convolution effects and data reconstruction. *Astron Astrophys*. **485**, 765–772 (2008).
28. Green, K.M., Borrás, M.C., Woskov, P.P., Flores, III, G.J., Hadidi, K., Thomas, P. Electronic excitation temperature profiles in an air microwave plasma torch. *IEEE Trans Plasma Sci*. **29**, 399–406 (2001).
29. Bendinelli, O. Abel integral equation inversion and deconvolution by multi-Gaussian

approximation. *Astrophys J*. **366**, 599–604 (1991).
30. Dörband, B., Müller, H., Gross, H. *Vol. 5 Metrology of Optical Components and Systems*, in H. Gross (ed.), *Handbook of Optical System*. Wiley-VCH (2012).
31. Sheikholeslami, M., Rokni, H.B. Simulation of nanofluid heat transfer in presence of magnetic field: A review. *Int J Heat Mass Trans*. **115**, 1203–1233 (2017).
32. Häfeli, U., Schütt, W., Teller, J., Zborowski, M. *Scientific and Clinical Applications of Magnetic Carriers*. Springer Science and Business Media (2013).

Figure 1

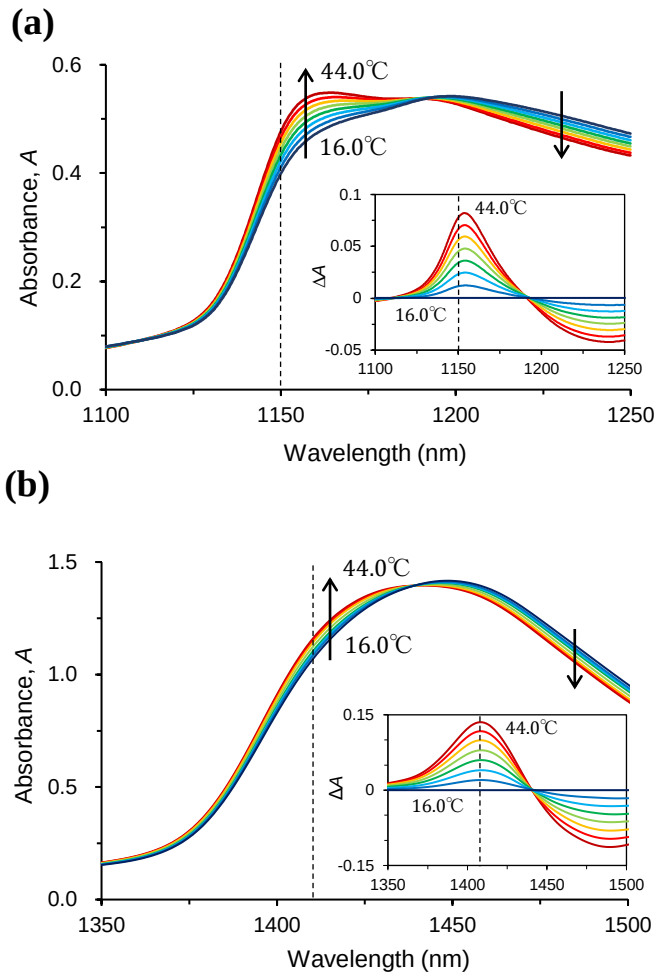

Figure 2

Click here to download Figure Fig2(Concept-coordinates)-kakuta-v1.pdf

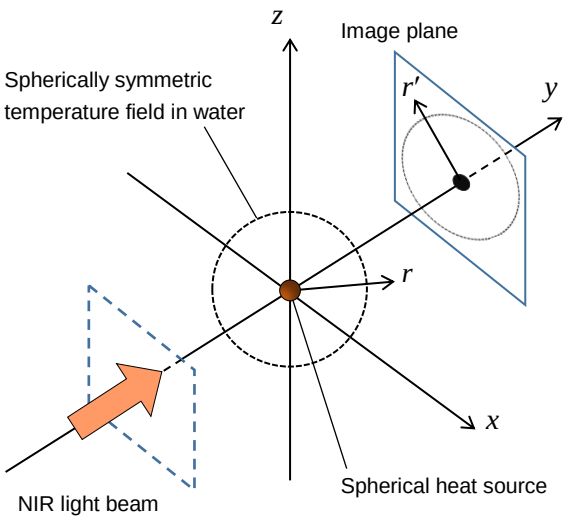

Figure 3

Click here to download Figure Fig3(Exp-system)-kakuta-v3.pdf

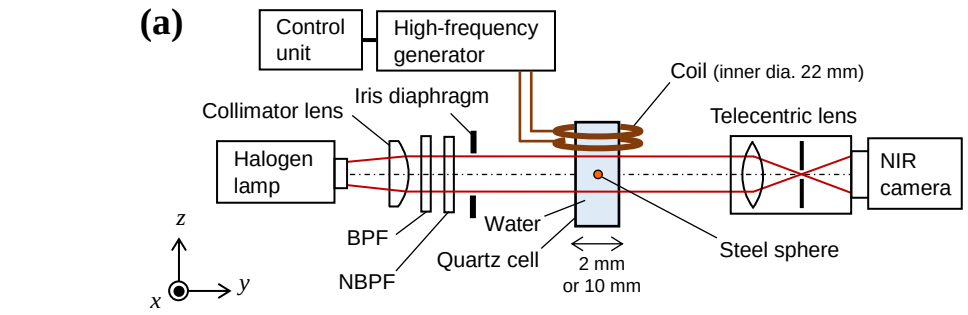

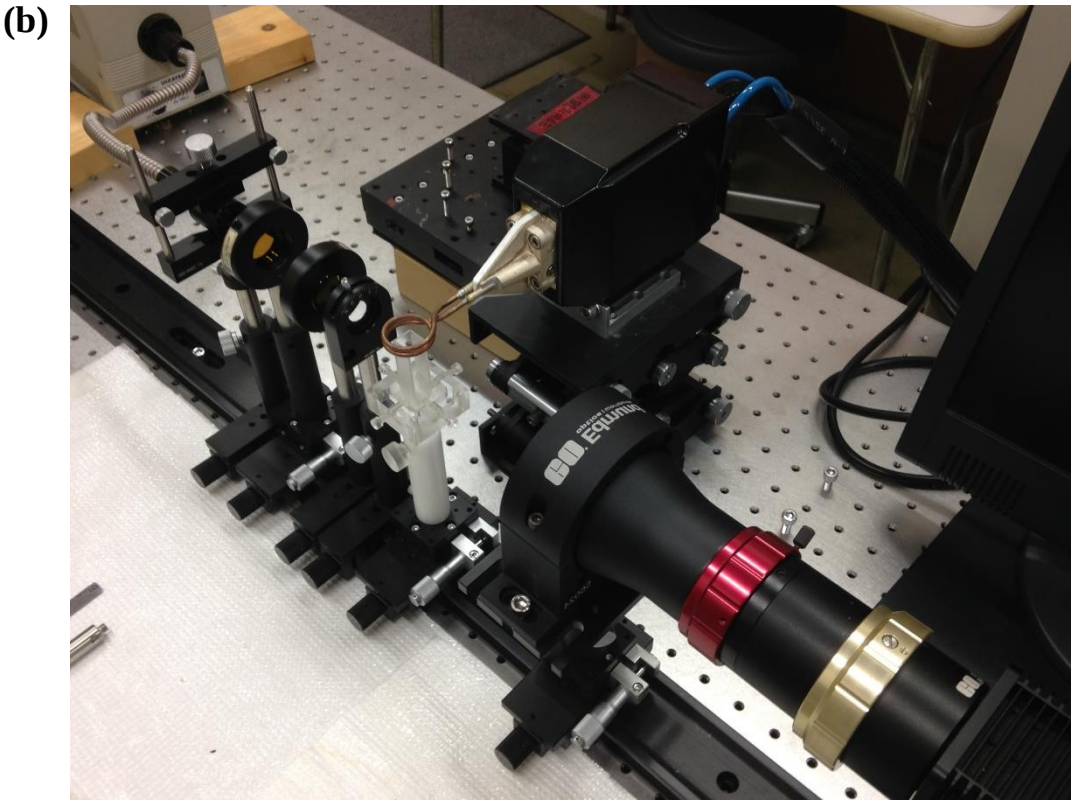

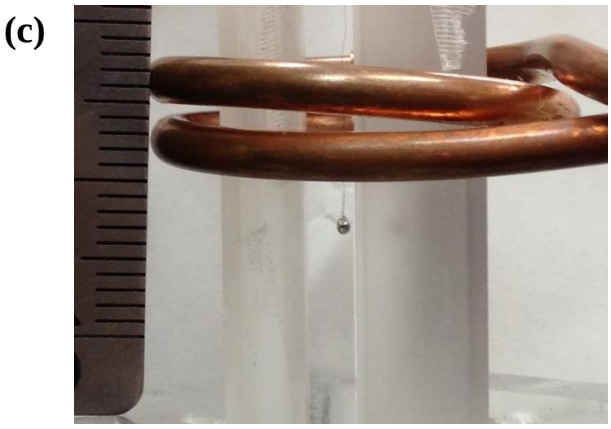

Figure 4

Click here to download Figure Fig4(I-images)-kakuta-v1.pdf

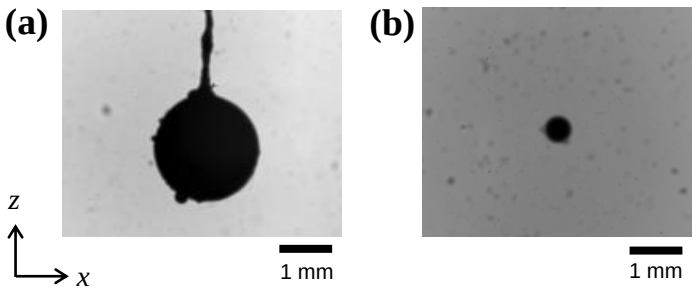

Figure 5

Click here to download Figure Fig5(DA-images-2mm)-kakuta-v3.pdf

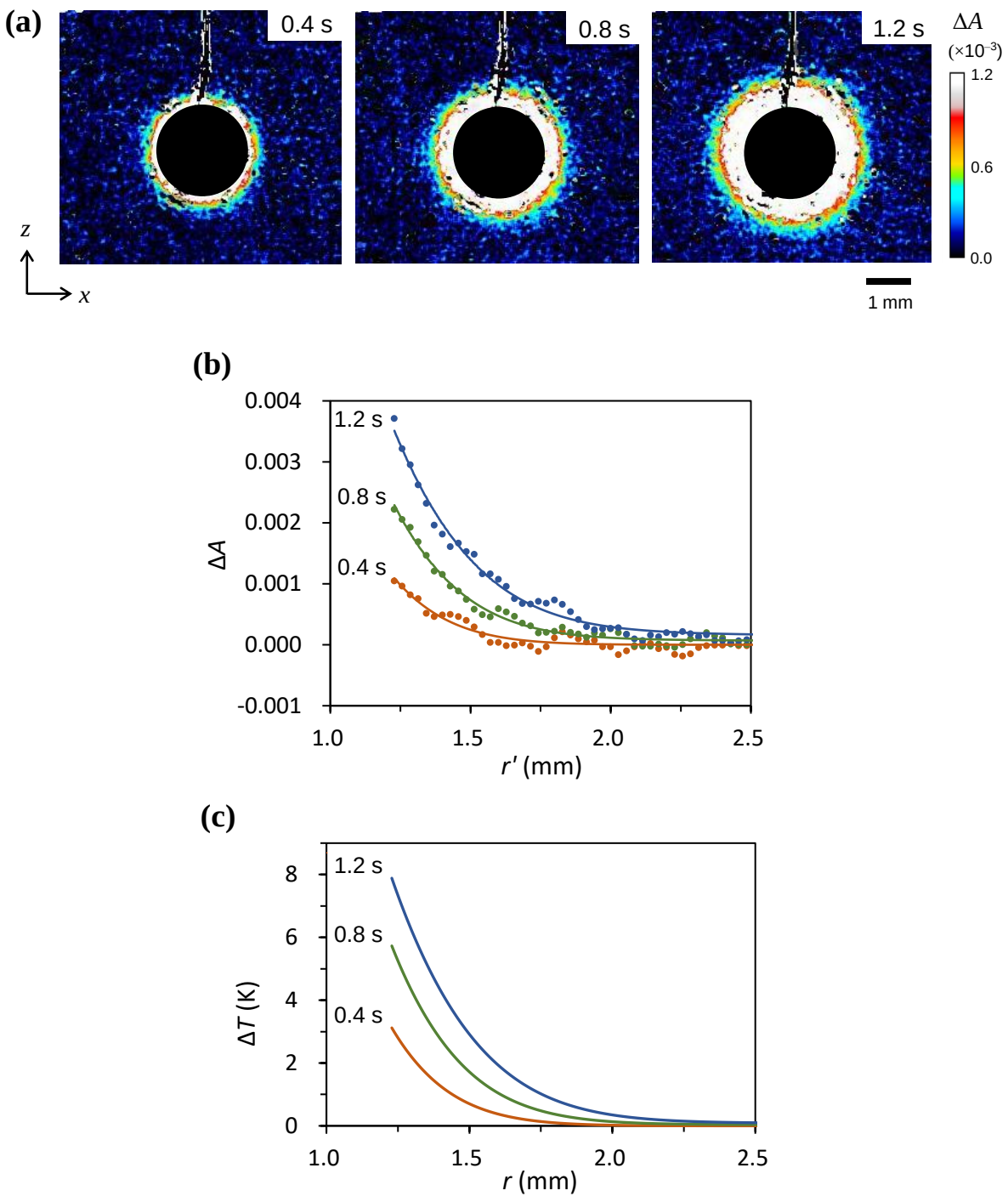

Figure 6

Click here to download Figure Fig6(DA-images-0.5mm)-kakuta-v2.pdf

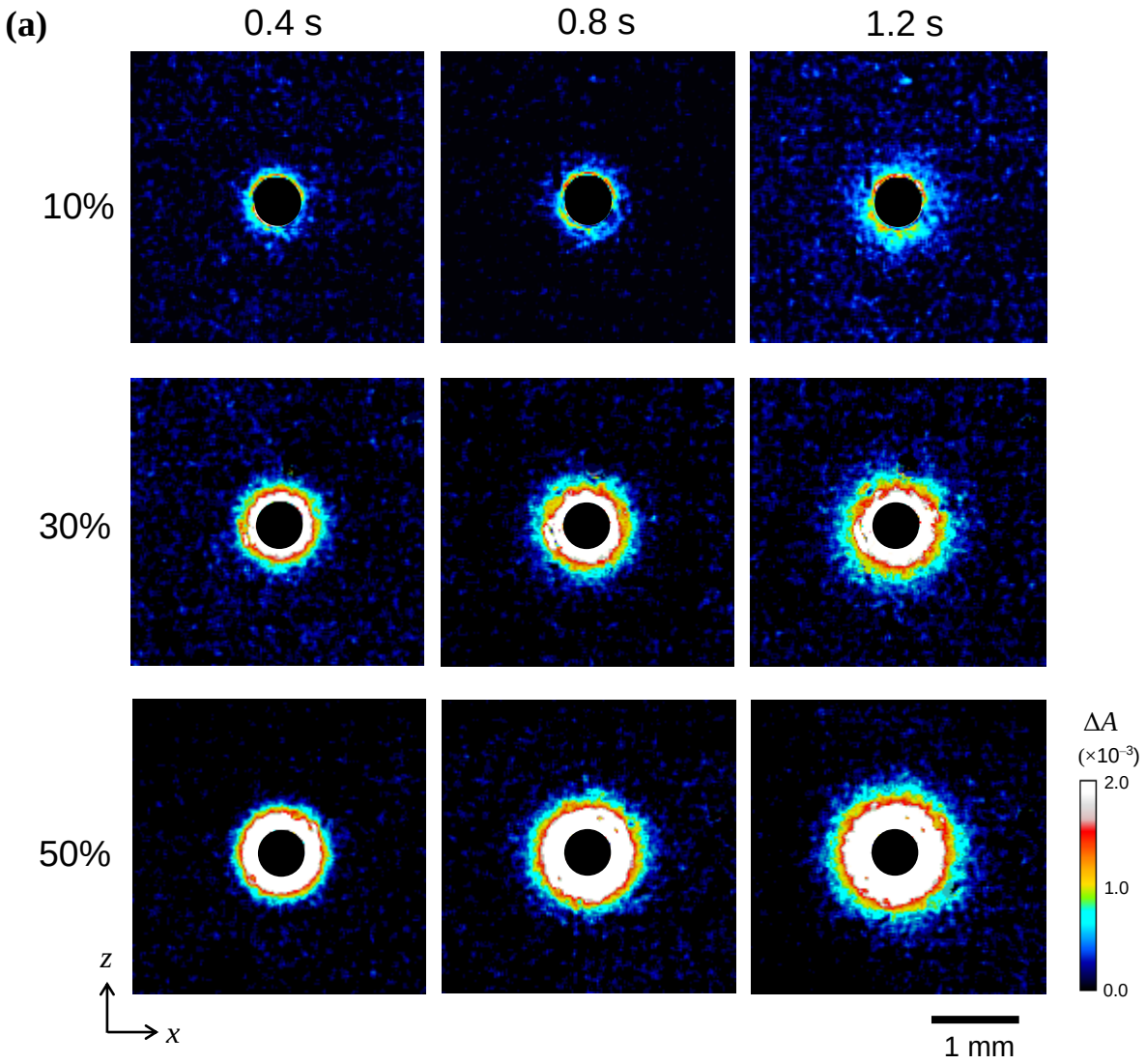

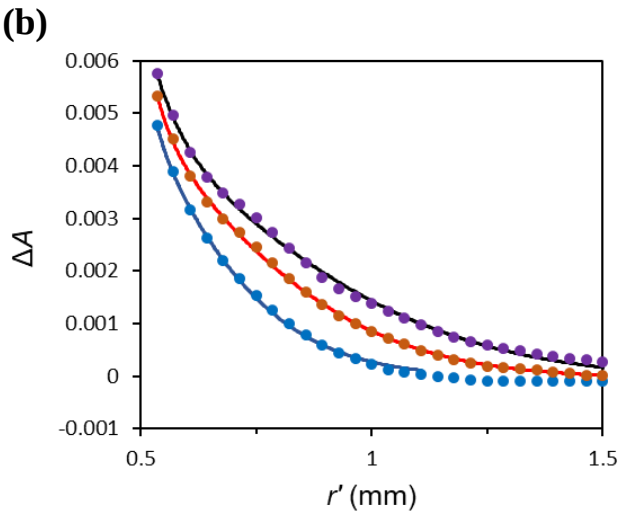

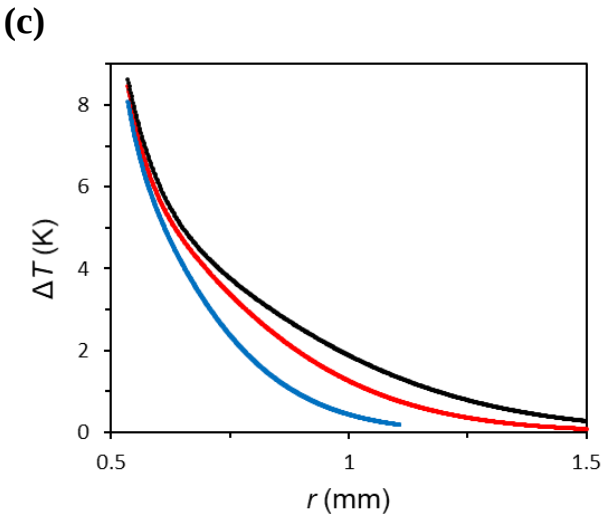

Materials Table

Click here to download Materials Table JoVE_Materials-v2.xls

Name of Material/ Equipment	Company	Catalog Number	Comments/Description
Induction heating system	CEIA, Italy	SPW900/56	780 kHz, 5.6 kW (max).
Coil	SA-Japan	custom	Water-cooled copper tube; two-turn; outer di
Water chiller	Matsumoto Kikai, Japan	MP-401CT	
Halogen lamp	Hayashi Watch-Works, Japan	LA-150UE-A	
Narrow bandpass filter for λ = 1150 nm	Andover	115FS10-25	Full width at half-maximum (FWHM): 10 nm.
Narrow bandpass filter for λ = 1412 nm	Andover	semi-custom	Full width at half-maximum (FWHM): 10 nm.
Bandpass filter for λ = 850–1300 nm	Spectrogon	SP-1300	
Bandpass filter for λ = 1100–2000 nm	Spectrogon	SP-2000	
NIR camera	FLIR Systems	Alpha NIR	InGaAs
Image acquisition software	FLIR Systems	IRvista	
Image processing software	NIH	ImageJ	ver. 1.51r
Image processing software	MathWorks	Matlab	ver. 2016a
Telecentric lens	Edmond Optics	55350-L	X1
Steel sphere (0.5 mm dia.)	Kobe Steel, Japan		Fe-1.5Cr-1.0C-0.4Mn (wt %)
Steel sphere (2.0 mm dia.)	Kobe Steel, Japan		Fe-1.5Cr-1.0C-0.4Mn (wt %)
Maltose syrup as aqueous gel	Sonton, Japan	Mizuame	Food product

a. 28 mm.

1 Alewife Center #200
Cambridge, MA 02140
tel. 617.945.9051
www.jove.com

ARTICLE AND VIDEO LICENSE AGREEMENT

Title of Article: A near-infrared temperature measurement technique for water surrounding an induction-heated small magnetic sphere

Author(s): Naoto Kakuta, Keisuke Nishijima, Van Cuong Han, Yuki Arakawa, Katsuya Kondo, Yukio Yamada

Item 1 (check one box): The Author elects to have the Materials be made available (as described at http://www.jove.com/author) via: [x] Standard Access [ ] Open Access

Item 2 (check one box):

[x] The Author is NOT a United States government employee.

[ ] The Author is a United States government employee and the Materials were prepared in the course of his or her duties as a United States government employee.

[ ] The Author is a United States government employee but the Materials were NOT prepared in the course of his or her duties as a United States government employee.

ARTICLE AND VIDEO LICENSE AGREEMENT

1. Defined Terms. As used in this Article and Video License Agreement, the following terms shall have the following meanings: "**Agreement**" means this Article and Video License Agreement; "**Article**" means the article specified on the last page of this Agreement, including any associated materials such as texts, figures, tables, artwork, abstracts, or summaries contained therein; "**Author**" means the author who is a signatory to this Agreement; "**Collective Work**" means a work, such as a periodical issue, anthology or encyclopedia, in which the Materials in their entirety in unmodified form, along with a number of other contributions, constituting separate and independent works in themselves, are assembled into a collective whole; "**CRC License**" means the Creative Commons Attribution-Non Commercial-No Derivs 3.0 Unported Agreement, the terms and conditions of which can be found at: http://creativecommons.org/licenses/by-nc-nd/3.0/legalcode; "**Derivative Work**" means a work based upon the Materials or upon the Materials and other pre-existing works, such as a translation, musical arrangement, dramatization, fictionalization, motion picture version, sound recording, art reproduction, abridgment, condensation, or any other form in which the Materials may be recast, transformed, or adapted; "**Institution**" means the institution, listed on the last page of this Agreement, by which the Author was employed at the time of the creation of the Materials; "**JoVE**" means MyJove Corporation, a Massachusetts corporation and the publisher of *The Journal of Visualized Experiments;* "**Materials**" means the Article and / or the Video; "**Parties**" means the Author and JoVE; "**Video**" means any video(s) made by the Author, alone or in conjunction with any other parties, or by JoVE or its affiliates or agents, individually or in collaboration with the Author or any other parties, incorporating all or any portion of the Article, and in which the Author may or may not appear.

2. Background. The Author, who is the author of the Article, in order to ensure the dissemination and protection of the Article, desires to have the JoVE publish the Article and create and transmit videos based on the Article. In furtherance of such goals, the Parties desire to memorialize in this Agreement the respective rights of each Party in and to the Article and the Video.

3. Grant of Rights in Article. In consideration of JoVE agreeing to publish the Article, the Author hereby grants to JoVE, subject to **Sections 4** and **7** below, the exclusive, royalty-free, perpetual (for the full term of copyright in the Article, including any extensions thereto) license (a) to publish, reproduce, distribute, display and store the Article in all forms, formats and media whether now known or hereafter developed (including without limitation in print, digital and electronic form) throughout the world, (b) to translate the Article into other languages, create adaptations, summaries or extracts of the Article or other Derivative Works (including, without limitation, the Video) or Collective Works based on all or any portion of the Article and exercise all of the rights set forth in (a) above in such translations, adaptations, summaries, extracts, Derivative Works or Collective Works and (c) to license others to do any or all of the above. The foregoing rights may be exercised in all media and formats, whether now known or hereafter devised, and include the right to make such modifications as are technically necessary to exercise the rights in other media and formats. If the "Open Access" box has been checked in **Item 1** above, JoVE and the Author hereby grant to the public all such rights in the Article as provided in, but subject to all limitations and requirements set forth in, the CRC License.

4. Retention of Rights in Article. Notwithstanding the exclusive license granted to JoVE in **Section 3** above, the Author shall, with respect to the Article, retain the non-exclusive right to use all or part of the Article for the non-commercial purpose of giving lectures, presentations or teaching classes, and to post a copy of the Article on the Institution's website or the Author's personal website, in each case provided that a link to the Article on the JoVE website is provided and notice of JoVE's copyright in the Article is included. All non-copyright intellectual property rights in and to the Article, such as patent rights, shall remain with the Author.

5. Grant of Rights in Video – Standard Access. This **Section 5** applies if the "Standard Access" box has been checked in **Item 1** above or if no box has been checked in **Item 1** above. In consideration of JoVE agreeing to produce, display or otherwise assist with the Video, the Author hereby acknowledges and agrees that, Subject to **Section 7** below, JoVE is and shall be the sole and exclusive owner of all rights of any nature, including, without limitation, all copyrights, in and to the Video. To the extent that, by law, the Author is deemed, now or at any time in the future, to have any rights of any nature in or to the Video, the Author hereby disclaims all such rights and transfers all such rights to JoVE.

6. Grant of Rights in Video – Open Access. This **Section 6** applies only if the "Open Access" box has been checked in **Item 1** above. In consideration of JoVE agreeing to produce, display or otherwise assist with the Video, the Author hereby grants to JoVE, subject to **Section 7** below, the exclusive, royalty-free, perpetual (for the full term of copyright in the Article, including any extensions thereto) license (a) to publish, reproduce, distribute, display and store the Video in all forms, formats and media whether now known or hereafter developed (including without limitation in print, digital and electronic form) throughout the world, (b) to translate the Video into other languages, create adaptations, summaries or extracts of the Video or other Derivative Works or Collective Works based on all or any portion of the Video and exercise all of the rights set forth in (a) above in such translations, adaptations, summaries, extracts, Derivative Works or Collective Works and (c) to license others to do any or all of the above. The foregoing rights may be exercised in all media and formats, whether now known or hereafter devised, and include the right to make such modifications as are technically necessary to exercise the rights in other media and formats. For any Video to which this Section 6 is applicable, JoVE and the Author hereby grant to the public all such rights in the Video as provided in, but subject to all limitations and requirements set forth in, the CRC License.

7. Government Employees. If the Author is a United States government employee and the Article was prepared in the course of his or her duties as a United States government employee, as indicated in **Item 2** above, and any of the licenses or grants granted by the Author hereunder exceed the scope of the 17 U.S.C. 403, then the rights granted hereunder shall be limited to the maximum rights permitted under such statute. In such case, all provisions contained herein that are not in conflict with such statute shall remain in full force and effect, and all provisions contained herein that do so conflict shall be deemed to be amended so as to provide to JoVE the maximum rights permissible within such statute.

8. Likeness, Privacy, Personality. The Author hereby grants JoVE the right to use the Author's name, voice, likeness, picture, photograph, image, biography and performance in any way, commercial or otherwise, in connection with the Materials and the sale, promotion and distribution thereof. The Author hereby waives any and all rights he or she may have, relating to his or her appearance in the Video or otherwise relating to the Materials, under all applicable privacy, likeness, personality or similar laws.

9. Author Warranties. The Author represents and warrants that the Article is original, that it has not been published, that the copyright interest is owned by the Author (or, if more than one author is listed at the beginning of this Agreement, by such authors collectively) and has not been assigned, licensed, or otherwise transferred to any other party. The Author represents and warrants that the author(s) listed at the top of this Agreement are the only authors of the Materials. If more than one author is listed at the top of this Agreement and if any such author has not entered into a separate Article and Video License Agreement with JoVE relating to the Materials, the Author represents and warrants that the Author has been authorized by each of the other such authors to execute this Agreement on his or her behalf and to bind him or her with respect to the terms of this Agreement as if each of them had been a party hereto as an Author. The Author warrants that the use, reproduction, distribution, public or private performance or display, and/or modification of all or any portion of the Materials does not and will not violate, infringe and/or misappropriate the patent, trademark, intellectual property or other rights of any third party. The Author represents and warrants that it has and will continue to comply with all government, institutional and other regulations, including, without limitation all institutional, laboratory, hospital, ethical, human and animal treatment, privacy, and all other rules, regulations, laws, procedures or guidelines, applicable to the Materials, and that all research involving human and animal subjects has been approved by the Author's relevant institutional review board.

10. JoVE Discretion. If the Author requests the assistance of JoVE in producing the Video in the Author's facility, the Author shall ensure that the presence of JoVE employees, agents or independent contractors is in accordance with the relevant regulations of the Author's institution. If more than one author is listed at the beginning of this Agreement, JoVE may, in its sole discretion, elect not take any action with respect to the Article until such time as it has received complete, executed Article and Video License Agreements from each such author. JoVE reserves the right, in its absolute and sole discretion and without giving any reason therefore, to accept or decline any work submitted to JoVE. JoVE and its employees, agents and independent contractors shall have

full, unfettered access to the facilities of the Author or of the Author's institution as necessary to make the Video, whether actually published or not. JoVE has sole discretion as to the method of making and publishing the Materials, including, without limitation, to all decisions regarding editing, lighting, filming, timing of publication, if any, length, quality, content and the like.

11. Indemnification. The Author agrees to indemnify JoVE and/or its successors and assigns from and against any and all claims, costs, and expenses, including attorney's fees, arising out of any breach of any warranty or other representations contained herein. The Author further agrees to indemnify and hold harmless JoVE from and against any and all claims, costs, and expenses, including attorney's fees, resulting from the breach by the Author of any representation or warranty contained herein or from allegations or instances of violation of intellectual property rights, damage to the Author's or the Author's institution's facilities, fraud, libel, defamation, research, equipment, experiments, property damage, personal injury, violations of institutional, laboratory, hospital, ethical, human and animal treatment, privacy or other rules, regulations, laws, procedures or guidelines, liabilities and other losses or damages related in any way to the submission of work to JoVE, making of videos by JoVE, or publication in *JoVE* or elsewhere by JoVE. The Author shall be responsible for, and shall hold JoVE harmless from, damages caused by lack of sterilization, lack of cleanliness or by contamination due to the making of a video by JoVE its employees, agents or independent contractors. All sterilization, cleanliness or decontamination procedures shall be solely the responsibility of the Author and shall be undertaken at the Author's expense. All indemnifications provided herein shall include JoVE's attorney's fees and costs related to said losses or damages. Such indemnification and holding harmless shall include such losses or damages incurred by, or in connection with, acts or omissions of JoVE, its employees, agents or independent contractors.

12. Fees. To cover the cost incurred for publication, JoVE must receive payment before production and publication the Materials. Payment is due in 21 days of invoice. Should the Materials not be published due to an editorial or production decision, these funds will be returned to the Author. Withdrawal by the Author of any submitted Materials after final peer review approval will result in a US$1,200 fee to cover pre-production expenses incurred by JoVE. If payment is not received by the completion of filming, production and publication of the Materials will be suspended until payment is received.

13. Transfer, Governing Law. This Agreement may be assigned by JoVE and shall inure to the benefits of any of JoVE's successors and assignees. This Agreement shall be governed and construed by the internal laws of the Commonwealth of Massachusetts without giving effect to any conflict of law provision thereunder. This Agreement may be executed in counterparts, each of which shall be deemed an original, but all of which together shall be deemed to me one and the same agreement. A signed copy of this Agreement delivered by facsimile, e-mail or other means of electronic transmission shall be deemed to have the same legal effect as delivery of an original signed copy of this Agreement.

A signed copy of this document must be sent with all new submissions. Only one Agreement required per submission.

CORRESPONDING AUTHOR:

Name:	Naoto Kakuta
Department:	Mechanical Engineering
Institution:	Tokyo Metropolitan University
Article Title:	A near-infrared temperature measurement technique for water surrounding an induction-heated small magne
Signature:	Naoto Kakuta
Date:	October 2nd, 2017.

Please submit a signed and dated copy of this license by one of the following three methods:

1) Upload a scanned copy of the document as a pfd on the JoVE submission site;
2) Fax the document to +1.866.381.2236;
3) Mail the document to JoVE / Attn: JoVE Editorial / 1 Alewife Center #200 / Cambridge, MA 02139

For questions, please email submissions@jove.com or call +1.617.945.9051

To Editors,

We, the authors have revised the manuscript according to the following editorial comments. The added and modified texts have been written in red. Also, Table of materials has been revised.

Editorial comments:

Note that some formatting changes and proofreading have already been done. Please proofread further to minimize spelling, grammar, and usage errors.
1.2.4: This is in Figure 3, but could you say where in the text as well?
1.2.6: Does this need to be focused or otherwise set up?
1.3.1: Please provide a little more information about this setup, including parameters for the generator.
1.3.3: The note here is a partial sentence; what is the distance supposed to be? What are its usual limits?
1.4.2: How, exactly, is induction heating started? Also, within 1 s of image storage?
2: Note that we will likely not be able to film these steps as a protocol; however, you will likely be able to explain the data analysis steps in the Results portion of the video.
2.1.5: What does ‘properly’ mean?
Figure legends: Please provide titles (in bold) for each figure here.

Figure permissions

Click here to download Supplemental File (Figures, Permissions, etc.) Email-AIP_for_reuse.docx

2017-11-21 1:44 GMT+09:00 AIPRights Permissions <Rights@aip.org>:

> Dear Dr. Kakuta:
>
> The document you attached is meant to be publishing agreement between you and AIP Publishing. The form cannot be used for authorizing permissions.
>
> However, we are happy to acknowledge and approve of your request to reuse figures from your previously published article in a new work.
>
> Permission is granted subject to these conditions:
>
> 1. AIP Publishing grants you non-exclusive world rights in all languages and media. This permission extends to all subsequent and future editions of the new work.
>
> 2. The following notice must appear with the material (please fill in the citation information):
>
> "Reproduced from [FULL CITATION], with the permission of AIP Publishing."
>
> When reusing figures, photographs, covers, or tables, the notice may appear in the caption or in a footnote. When reusing a full article, the notice must be printed on the first page of the reprinted article or book chapter.
>
> In cases where the new publication is licensed under a Creative Commons license, the full notice as stated above must appear with the reproduced material.
>
> 3. If the material is published in electronic format, we ask that a link be created pointing back to the abstract of the article on the journal website using the article's DOI.
>
> 4. This permission does not apply to any materials credited to another source.
>
> Please let us know if you have any questions.
>
> Sincerely,
> Susann Brailey
> Manager, Rights & Permissions
>

> AIP Publishing
> 1305 Walt Whitman Road | Suite 300 | Melville NY 11747-4300 | USA
> t +1.516.576.2268
> rights@aip.org | publishing.aip.org
> Follow us: Facebook | Twitter | LinkedIn
>
>

Supplemental File 1 (Figure)

Click here to download Supplemental File (Figures, Permissions, etc.) Supplement1(Image-processing)-kakuta-v2.pdf

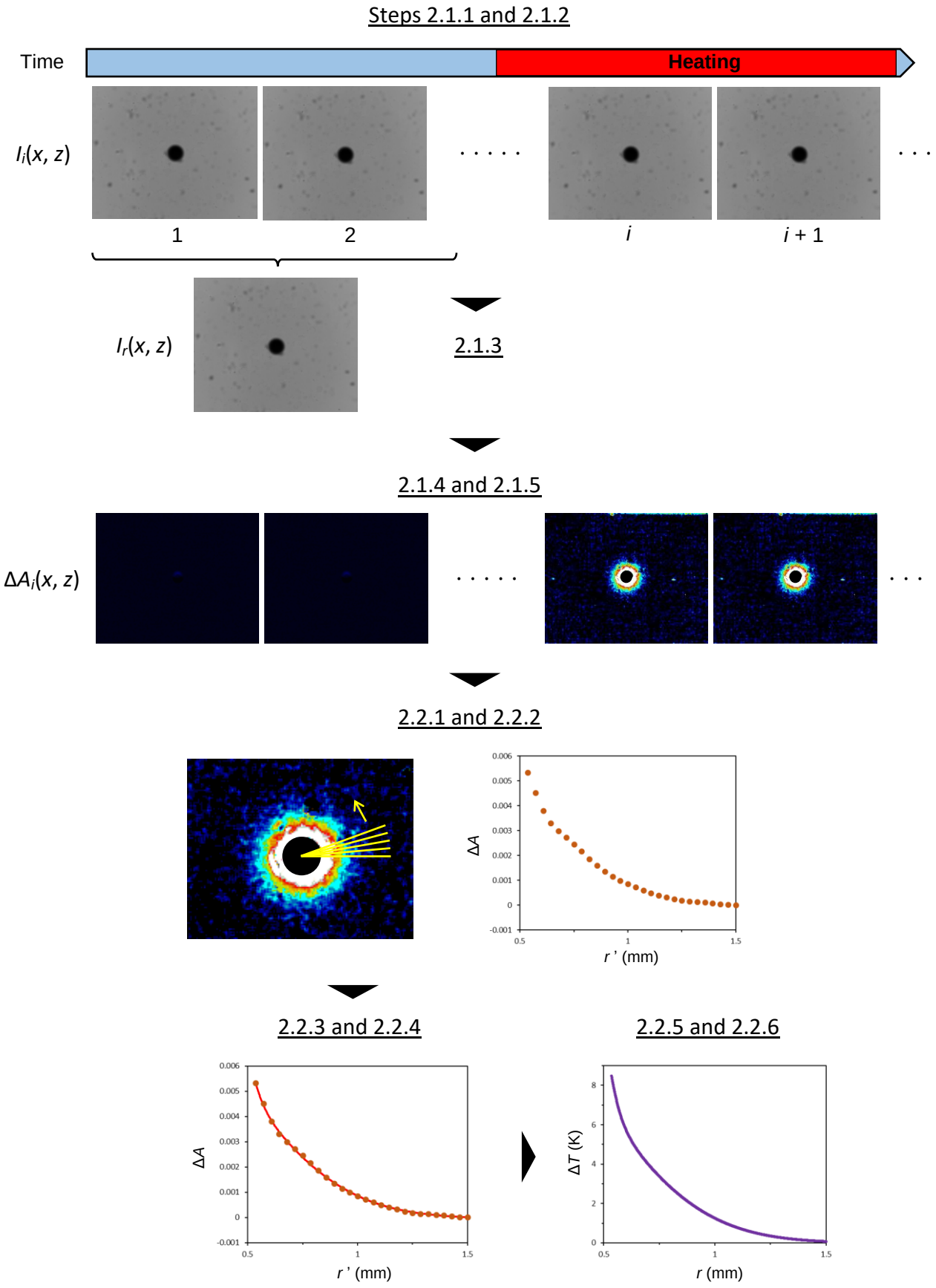

Supplemental File 2 (Program code)

Click here to download Supplemental File (Figures, Permissions, etc.) Supplement2(Macro-image).txt

```
// Macro for ImageJ:
// Construction of absorbance differnce images from intensity images
// by Naoto Kakuta, Tokyo Metropolitan University 2017/11/30.

//Slice (frame) number used for reference intensity (Iref) construction
srefmin = 2; //minimum slice number
srefmax = 5; //maximum slice number

//File name of current intensity (I) images (stack Tiff)
diri = getDirectory("image");  //directory of I image
fni = getTitle; //file name of I image
pathi = diri+fni; //path of I image

//File name of absorbance difference (DA) images (stack Tiff)
dira = diri; //directory of DA image = directory of current image
fna = "da-"+fni; //file name of DA image
patha = dira+fna; //path of DA image

//Smoothing
run("Multiply...", "value=16 stack"); //12-bit(0-4095) to 16-bit(0-65520)
run("Smooth", "stack"); //3x3 pixel smoothing

//Iref definision
run("Z Project...", "start="+srefmin+" stop="+srefmax+"
projection=[Average Intensity]"); //averaging

//DA calculation
imageCalculator("Divide create 32-bit stack", fni,"AVG_"+fni); //=I/Iref
run("Log", "stack"); //=ln(I/Iref)
run("Multiply...", "value=-0.434300 stack"); //=-log10(I/Iref) = DA

//Save and display
run("Save", "save=["+patha+"]"); //save DA image as stack Tiff

close();
close();
close();

open(patha); //open DA image stack
run("Royal"); //colorization (Royal)
//run("Jet"); //colorization (Jet)

//
//------ END -------
```

```
// Macro for ImageJ:
// Averaging of absorbance line profiles over different angles //
// by Naoto Kakuta, Tokyo Metropolitan University 2017/11/30.
//
//------- Input parameters -------
//
// File name for save
fn = "C:\\Users\\kakuta\\Desktop\\radial-profile.txt";

// Center of circle in pixel number
x0 = 158; //x-coordinate
y0 = 125; //y-coordinate

// Radius range (numbers of pixel from the center)
rmin = 15; //minimum pixel number
rmax = 80; //maximum pixel number

// Exclusion of angle range in degree (if nothing, assign 0)
thmin = 80; //minimm angle
thmax = 100; //maxmum angle

// Selection of slice (frame) numbers in stack
slmin = 45; //minimum slice number
slmax = 120; //maximum slice number
// If all slices are selected, use:
// slmin = 1;
// slmax = nSlices;
//
//------- Processing commands (Do not modify) -------
//
jmax =rmax-rmin+1; //total pixel number of radial line
dth = 2*PI/360;          //angle step in radian (1 degree)
thmin = thmin/360*2*PI; //conversion to radian
thmax = thmax/360*2*PI; //conversion to radian
value = newArray(jmax); //definition of 1D-array "value"

//number of lines
sumk = 0;
for(k=0; k<360; k++){
theta = k*dth; //angle of radial line
if(theta <= thmin || theta >= thmax)
sumk = sumk + 1; //total number of radial lines
}

for(i=0; i<(slmax-slmin+1); i++){
  currentslice = slmin + i; //slice number
  setSlice(currentslice); //set the slice
  print("frame No.",currentslice);
  Array.fill(value,0); //reset value (=0)

  for(j=0; j<jmax; j++){
    r = rmin + j; //radius of point (x,y) in pixel unit

    for(k=0; k<360; k++){
```

```
      theta = k*dth; //angle in radian
      valuet = 0; //temporal value

      if(theta <= thmin || theta >= thmax){
        x = r*cos(theta); //x-coordinate of the point
        y = r*sin(theta); //y-coordinate of the point

//-- Weight averaging using surrounding 4 pixels --
//      Pixel(x2,y2)         Pixel(x1,y1)
//                    (x,y)
//      Pixel(x3,y3)         Pixel(x4,y4)
//
        x1 = floor(x) + x0 +1; //x-coordinate
        y1 = floor(y) + y0 +1; //y-coordinate
        x2 = x1 - 1;
        y2 = y1;
        x3 = x1 - 1;
        y3 = y1 - 1;
        x4 = x1;
        y4 = y1 - 1;
        d1 = sqrt((x1 - x)^2 + (y1 - y)^2); //distance between (x,y) and
(x1,y1)
        d2 = sqrt((x2 - x)^2 + (y2 - y)^2);
        d3 = sqrt((x3 - x)^2 + (y3 - y)^2);
        d4 = sqrt((x4 - x)^2 + (y4 - y)^2);
        if(d1 == 0)
          valuet = getPixel(x1,y1); //(x,y)=(x1,y1)
        else if(d2 == 0)
          valuet = getPixel(x2,y2);
        else if(d3 == 0)
          valuet = getPixel(x3,y3);
        else if(d4 == 0)
          valuet = getPixel(x4,y4);
        else{
          d1 = 1/d1;
          d2 = 1/d2;
          d3 = 1/d3;
          d4 = 1/d4;
          dsum = d1 + d2 + d3 + d4;
          value1 = getPixel(x1,y1);
          value2 = getPixel(x2,y2);
          value3 = getPixel(x3,y3);
          value4 = getPixel(x4,y4);
          valuet = d1*value1 + d2*value2 + d3*value3 + d4*value4;
//weighting
          valuet = valuet/dsum;
//---------------------------------
        }
      }
      value[j] = value[j] + valuet;
    }
    value[j] = value[j] / sumk;
    print(r,value[j]);
  }
```

```
}
saveAs("Text", fn); //file save
//
//------ END -------
```

Supplemental File 4 (Program code)